A General Method for Propagation of the Phase Space Distribution, with Application to the Sawtooth Instability [*]

Robert L. Warnock

Stanford Linear Accelerator Center, Stanford University, Stanford, CA 94309
E-mail: warnock@slac.stanford.edu

James A. Ellison

Department of Mathematics and Statistics, University of New Mexico
Albuquerque, NM 87131
E-mail: ellison@math.unm.edu

Abstract

We propose and illustrate a general numerical method to follow the probability distribution in phase space as a function of time. It applies to any multiparticle system governed by Liouville, Vlasov or Vlasov-Fokker-Planck dynamics. The technique, based on discretization of the local Perron-Frobenius operator, is simple in concept, easy to implement, and numerically stable in examples studied to date. We illustrate by treating longitudinal dynamics in electron storage rings with realistic wake field. Applied to the SLC damping rings, the method gives the observed current threshold for bunch lengthening, and several aspects of observed behavior above threshold, including the presence of a bursting or sawtooth mode. In contrast to previous particle-in-cell simulations, we have very low numerical noise and the ability to follow the motion over several damping times. The method has also been applied to the coherent beam-beam interaction. It appears likely that this approach will be of interest for some of the central problems of this workshop, for instance matching of space-charge dominated beams to a focusing channel, and coherent synchrotron radiation with self-consistent charge/current density.

1 Introduction

Coherent motion of particles in accelerator beams is described in probabilistic terms by means of a distribution function $f(z, t)$, where z is a point in phase space. It is often a good approximation to represent the interparticle interaction through the field produced by a smoothed charge-current distribution, neglecting the actual granularity of charge. In that case we can follow Vlasov, reducing the dimension of phase space for an N-particle system from $2dN$ to $2d$, where a single particle moves with d degrees of freedom. In this view $f(z, t)dz$ is the probability of finding a single particle (any one of the N) with phase point $z \in \mathbf{R}^{2d}$ in a volume element dz about z, and the charge-current vector for the collection of all particles is

$$(\rho, J) = eN \int (1, v(z)) f(z, t) dp , \tag{1}$$

where $v(z)$ is the Cartesian velocity associated with phase point $z = (q, p)$. Here q and p are d-component vectors representing canonical coordinates and momenta, respectively. Maxwell-Vlasov dynamics is defined by saying that the force on any particle due to other particles is the Lorentz force $e(E + v \times B)$, where E and B are the fields from Maxwell's equations with charge-current (1). We call this the *collective force*.

Conservation of probability requires that

$$f(z', t)dz' = f(z, 0)dz , \tag{2}$$

where the trajectory starting at z at time 0 evolves to z' at time t, and volume element dz evolves to dz'. If the system is Hamiltonian its time evolution is volume-preserving, $dz' = dz$. Then (2) implies that $f(z(t), t)$ is independent of t, where $z(t)$ is a particle trajectory. Putting $df(z(t), t)/dt = 0$ and applying Hamilton's equations we obtain Vlasov's nonlinear integro-partial-differential equation for f:

$$\frac{\partial f}{\partial t} + \frac{\partial f}{\partial q} \cdot \frac{\partial H}{\partial p} - \frac{\partial f}{\partial p} \cdot \frac{\partial H}{\partial q} = 0 , \tag{3}$$

where the Hamiltonian $H(z, t, f(\cdot, t)) = H_e(z, t) + H_c(z, t, f(\cdot, t))$ contains a term H_e accounting for external fields and a term H_c accounting for the collective force. (When we write $f(\cdot, t)$ as the argument of a function we mean that the function depends on $f(\zeta, t)$ for all ζ; for instance, there may be an integral over ζ in the definition of the function). Since H_c is a functional of f itself, this is a big generalization of the classical Hamiltonian function. The independent variable t may not be literally the time; in accelerator models it might be arc-length s on a reference trajectory, or the betatron phase, or distance along a curve in a local coordinate system. We retrieve the Liouville equation for non-interacting particles in the case $H_c = 0$.

If the system involves dissipation and fluctuations, as in the case of electrons producing synchrotron radiation, Eq.(3) must be augmented to include Fokker-Planck terms. In the simplest description one makes a sort of "smooth approximation" in which the dissipation and fluctuations are distributed homogeneously in the independent variable. In that picture the Fokker-Planck terms take the form presented in Chandrasekhar's classical exposition

2

[1] or in books of Gardiner [2], Risken [3], and Soize [4]. The fluctuations are described as increments of a Wiener process; i.e., the momemtum receives random kicks that have a Gaussian distribution, two kicks at different t or for different degrees of freedom being statistically independent [5, 6]. The augmented Vlasov equation with this minimal model of dissipation/fluctuation is

$$\frac{\partial f}{\partial t} + \frac{\partial f}{\partial q} \cdot \frac{\partial H}{\partial p} - \frac{\partial f}{\partial p} \cdot \frac{\partial H}{\partial q} = 2\beta \frac{\partial}{\partial p} \cdot (pf) + D \frac{\partial}{\partial p} \cdot \frac{\partial}{\partial p} f, \qquad (4)$$

where β is the damping rate, and D is the diffusion constant of the random process (assumed to be the same in all degrees of freedom). We call this the Vlasov-Fokker- Planck (VFP) equation, although in accelerator physics it is often called simply the Fokker-Planck equation. We avoid the latter name, since in other disciplines it refers to the original equation without the collective force.

For an accurate accelerator model one has to account for the fact that synchrotron radiation is localized at various places in the accelerator, takes place not only in bending magnets, is influenced by interplane (x-y) coupling, and so on. Also, synchrotron radiation is not the only source of noise. Such refinements have been treated by Jowett [7] and Ripken *et al.* [8]. For the simple model of the present work we shall be content with the description of Eq.(4).

Although Eq.(4) or its special case Eq.(3) would seem to provide a solid basis for a wide class of problems in accelerator physics, the analysis of its solutions is still in a primitive state. For many years the main application was in linear stability studies. Typically, one linearized the equation about some distribution f_0, and tried to see whether $f_1 = f - f_0$ would stay bounded or blow up as a function of time. Usually f_0 was supposed to be an equilibrium distribution of the nonlinear equation or an approximation thereto, but there is only one case that we know of in which an equilibrium was convincingly computed (numerically). That is the case of longitudinal motion in a storage ring, allowing an arbitrary longitudinal wake field, but with the essential assumption that the wake force is averaged over one turn, hence independent of s. In this model the equilibrium solution of the VFP equation is a solution of Haïssinski's [9] nonlinear integral equation. Under weak assumptions on the wake one can prove that this equation has a unique solution at sufficiently small current [10]. The solution is not difficult to compute numerically [10, 11], even at very large current. More general integral equations for equilibria have been studied in the mathematical literature [12] and by the authors in connection with the beam-beam problem [13].

The study of Oide and Yokoya [14] was the first in which the Vlasov equation was linearized about the Haïssinski solution. The linearization resulted in a linear integral equation in the frequency domain. Roots of its determinant in the upper-half frequency plane should correspond to linear instability of the Haïssinski equilibrium. There are unresolved mathematical and physical issues in this matter, however, since the integral equation is not a standard Fredholm equation for which a finite-dimensional approximation is assured. Rather, it is an integral equation of the third kind, which has solutions in a space of generalized functions [15], the van Kampen - Case singular solutions [16]. These can be treated rigorously by a slight generalization of the methods of Ref.[15], in which the mathematical problem is reduced to a Fredholm equation.

Direct numerical integration of the VFP equation in the time domain could, in principle, help to answer questions of existence and stability of equilibria, and even approach richer phenomena in which an instability "saturates" through nonlinear effects. We know of few previous attempts in this direction for accelerator problems, at least for the case of high-energy, low-emittance beams [17]. Rather, time-domain simulations normally are done by following an ensemble of macro-particles in configuration space, approximating the charge distribution by values on grid points to produce a source for the collective force. This is usually called the particle-in-cell (PIC) method [18]. It has the advantage of lower dimensionality, since it works in configuration space rather than phase space. One could, in principle, follow the granular distribution of macro-particles in phase space, even though it is not needed for the computation. Bane and Oide [19] have applied the PIC method to the same problem we treat in Sections 3 and 4, and have obtained results that anticipate ours in some qualitative aspects.

Plasma physicists [20, 21, 22, 23, 24] have reported time domain integration of the nonlinear Vlasov equation, and have remarked that, compared to PIC simulation, the technique offers lower noise and better load balancing in parallel computation [21, 22]. These authors are usually not interested in long-time behavior with weak damping and fluctuations, the problem of interest for electron storage rings. Nevertheless, we may be able to exploit part of the technique used successfully in plasma physics. Averaging methods have also been proposed for approximate solution of the Vlasov equation in beam physics [25].

On first sight it would seem that the equation could be approached by the usual methods for partial differential equations, for instance by using finite differences to approximate the q and p derivatives, thereby obtaining a large system of ordinary differential equations for unknowns $f(z_i, t)$, the z_i being nodes of a finite grid. Here one makes a corresponding discretization of integrals defining the collective force, by some numerical integration rule. It was surprising to find that such a technique fails utterly, with or without implicit time stepping, and not because of any effect of the nonlinear terms. Rather, it fails even for the simple Liouville equation for an harmonic oscillator! The failure is immediate and catastrophic: spurious oscillations appear on the tails of the distribution and quickly grow without bound, all within a time less than the period of the harmonic motion. A spectral method, based on expansion in Hermite polynomials, had similar bad behavior. To escape from this disgraceful situation, we first looked for a method that would solve the harmonic oscillator problem. Having found one, only small embellishments were required to solve the full nonlinear VFP equation.

2   Approximating the Perron-Frobenius Operator

Our heuristic understanding of the failure of the finite difference method is that it pays too little attention to the primary conservation equation (2). This comes to light when we recall that an explicit representation of the solution of the Liouville problem follows directly from (2). If we fail to exploit that representation we are only making life difficult. Suppose that the single-particle motion under the Hamiltonian H_e alone is given by a map M, which may

be nonlinear. We write
$$z' = M(t_2|t_1)(z) \; , \tag{5}$$
implying that the trajectory passing through z at time t_1 passes through z' at time t_2. Then (2) implies
$$f(M(t|0)(z), t) = f(z, 0) \; . \tag{6}$$
Replacing z in this equation by $M(t|0)^{-1}(z) = M(0|t)(z)$ we see that
$$f(z, t) = f(M(0|t)(z), 0). \tag{7}$$

For an arbitrary initial distribution $f(z, 0) = f_0(z)$ this formula solves the initial value problem of the independent-particle Liouville equation for $H = H_e$.

The Perron-Frobenius (PF) operator $\mathcal{M}$ associated with a volume preserving map M is defined by its action on an arbitrary function $g(z)$ in the following way [26]:
$$\mathcal{M}g(z) = g(M^{-1}(z)) \; . \tag{8}$$

This is a linear operator since

$$\mathcal{M}(g_1 + g_2)(z) = (g_1 + g_2)(M^{-1}(z)) =$$
$$g_1(M^{-1}(z)) + g_2(M^{-1}(z)) = \mathcal{M}g_1(z) + \mathcal{M}g_2(z) \; . \tag{9}$$

Writing $\mathcal{M}(t|0)$ for the PF operator associated with $M(t|0)$ we see that the solution of the Liouville equation is just the PF operator applied to the initial distribution:
$$f(z, t) = \mathcal{M}(t|0)f_0(z) \; . \tag{10}$$

One can hope to extend this idea to the nonlinear Vlasov case by supposing that the collective force can be regarded as an external force over a sufficiently small time interval Δt. One then has a map $M(t + \Delta t|t)_{f(\cdot,t)}$, which depends on f evaluated at time t, and which gives the evolution of f for a small time step as

$$f(z, t + \Delta t) \approx f(M(t|t + \Delta t)_{f(\cdot,t)}(z) \; , \; t) = \mathcal{M}_{f(\cdot,t)}(t + \Delta t|t)f(z, t) \; . \tag{11}$$

We refer to the $\mathcal{M}$ of this equation as the *local* Perron- Frobenius operator, to emphasize that its corresponding map M varies as f evolves in time. To avoid notational clutter, we shall suppress the subscript $f(\cdot, t)$ in the sequel.

To apply (11) in a computation with successive time steps Δt we need a suitable discretization, which is to say a finite-dimensional representation of the z-dependence of the unknown f. For instance, suppose we assume a truncated orthonormal expansion

$$f(z, t) \approx \sum_{m=0}^{\overline{m}} f_m(t)\phi_m(z) \; . \tag{12}$$

5

Then, reflecting the linear nature of the PF operator, the time evolution expressed in (11) is given as a linear transformation on the expansion coefficients:

$$f_m(t + \Delta t) \approx \sum_{n=0}^{\overline{m}} \mu_{mn} f_n(t) \ ,$$

$$\mu_{mn} = \int \phi_m^*(z) \phi_n(M(t|t + \Delta)(z)) dz \ . \tag{13}$$

Here there are two levels of approximation, one from the assumption of a locally time-independent collective force in (11) and the other from the truncation in (12). Provided that we choose a volume preserving (e.g., symplectic) representation of $M(t + \Delta t|t)$ the transformation (11) conserves probability, but there is a possible loss of probability conservation from approximation (12). In fact, conservation of the the total probability $\int f(z,t) dz$ provides a useful control on the accuracy of the computation.

Actually, we think that orthogonal expansion is probably an inefficient method. Local polynomial approximation of $f(z,t)$ in z seems more promising, and that is the technique we employ in the following.

If we adopt discretization of the local PF operator as the method to integrate the Vlasov equation, we still must deal with the Fokker-Planck terms. It turns out that an exceedingly simple method is effective for that. We invoke operator splitting, interleaving evolution by (11) with evolution by the Fokker-Planck (FP) operator for a step Δt. The latter is done by an elementary method for PDE integration, as explained in the following section. We have found in two examples (that of the following section and the beam-beam problem) that the resulting scheme is numerically stable over long times, allowing simulations over intervals equal to several damping times of typical storage rings. Moreover, we obtain excellent conservation of probability and very smooth distributions.

3   Example: Longitudinal Motion with Wake Field

We consider longitudinal motion in an electron storage ring with an arbitrary wake potential. We suppose that the synchrotron oscillations are in the linear region of the applied r.f. field. Following Ref.[14] we use normalized, dimensionless phase space variables q, p as follows:

$$q = \frac{z}{\sigma_z} \ , \qquad p = -\frac{E - E_0}{\sigma_E} \ , \tag{14}$$

where z is the distance from the synchronous particle, E is the energy, and E_0 the mean energy. We take $z = s - s_0$ to be positive for a particle in front of the synchronous particle. The quantities $\sigma_z = \langle z^2 \rangle^{1/2}$ and $\sigma_E = \langle (E - E_0)^2 \rangle^{1/2}$ are the rms bunch length and rms energy spread in the low-current equilibrium state without wake field. The electrons are assumed to be ultrarelativistic. We incorporate the well-known relation [27]

$$\sigma_z = \frac{\alpha c}{\omega_s E_0} \sigma_E \ , \tag{15}$$

6

where α is the momentum compaction factor and $\omega_s = 2\pi f_s$ is the synchrotron frequency. Using (15) one sees that the usual equations of motion for synchrotron motion [27, 28] are the same as Hamilton's equations for the Hamiltonian $H_e(q, p) = (q^2 + p^2)/2$; namely,

$$dq/d\theta = p , \quad dp/d\theta = -q , \quad \theta = \omega_s t . \tag{16}$$

Here t is the laboratory time. The collective force is taken to be

$$F(q, f(\cdot, \theta)) = \int_{-\infty}^{\infty} W(q - q')\left[\int_{-\infty}^{\infty} f(q', p, \theta)dp\right]dq' . \tag{17}$$

The wake potential $W(q - q')$ gives the longitudinal electric field (averaged over one turn) on a test particle at q due to a point source at q', expressed as a potential difference for one turn. That is, apart from a sign, the field is $W(q - q')/C$, where C is the circumference of the reference orbit. The sign of W is a matter of convention; we suppose that a positive value of W corresponds to energy gain. With this definition the complete Hamiltonian is $H_e + H_c$ where

$$H_c(q, f(\cdot, \theta)) = \quad -I \int_q^{\infty} F(q', f(\cdot, \theta))dq' \tag{18}$$

$$I = \quad \frac{Ne^2}{2\pi\nu_s\sigma_E} . \tag{19}$$

The number of particles is N, e is the electron charge, and ν_s is the synchrotron tune, $2\pi\nu_s = \omega_s T$ for revolution time T. The minus sign in (18) arises from the convention on W and the minus sign in the definition (14) of p. The expression for the beam current parameter I (not literally a current) is derived by translating the equation of motion $dp/d\theta = -\partial H/\partial q$ into $dP/dt = \mathcal{F}$, where $P = E/c$ and $\mathcal{F}$ are the physical momentum and force, respectively.

With the above definitions the VFP equation (4) for the present example takes the form

$$\frac{\partial f}{\partial \theta} + p\frac{\partial f}{\partial q} - (q + IF(q, f))\frac{\partial f}{\partial p} = \frac{\partial}{\partial p}(2\beta pf + D\frac{\partial f}{\partial p}) , \tag{20}$$

where β is the damping rate per radian of θ and D is the diffusion constant. We find that $D = 2\beta$ by the following argument. Consider the unperturbed case with $I = 0$. To find its equilibrium solution f_0 make the Ansatz $f_0(q, p) = f_0(q, -p)$, which has a physical basis in the condition of detailed balance [2]. Then the right side of (20) is even in p while the left side is odd, hence the two sides are separately zero. The general solution making the left side zero is $f_0(q, p) = \Phi(x)$, $x = (q^2 + p^2)/2$, for an arbitrary smooth function Φ. The condition for the right side to be zero as well is

$$2\beta\Phi(x) + D\Phi'(x) + p^2(2\beta\Phi'(x) + D\Phi''(x)) = 0 . \tag{21}$$

Since this must hold for all x at any p, in particular at $p = 0$, we see that $\Phi(x) = \text{const} \cdot \exp(-2\beta x/D)$, or

$$f_0(q, p) = \frac{1}{2\pi\sigma^2}\exp[-\frac{q^2 + p^2}{2\sigma^2}] , \quad \sigma^2 = \frac{D}{2\beta} . \tag{22}$$

Thus, in the unperturbed equilibrium state, $\sigma_q = \sigma_p = \sigma$, whereas the definitions (14) demand that $\sigma_q = \sigma_p = 1$, hence $D = 2\beta$.

To find the equilibrium solution $f(q, p)$ of the full problem (20) we again assume detailed balance, and note that the left side is zero if $f(q, p) = \Phi(H(q, p, f))$ for an arbitrary smooth Φ. Again, the right side being zero leads to $\Phi(x) = \text{const} \cdot \exp(-x)$. Thus,

$$f(q, p) = (2\pi)^{-1/2} \exp(-p^2/2)\rho(q) ,\qquad (23)$$

where the charge density ρ satisfies Haïssinski's integral equation [9],

$$\rho(q) = \frac{\exp[-q^2/2 + I \int_q^\infty F(q', \rho)dq']}{\int_{-\infty}^\infty dq \exp[-q^2/2 + I \int_q^\infty F(q', \rho)dq']},\qquad (24)$$

with

$$F(q, \rho) = \int_{-\infty}^\infty W(q - q')\rho(q')dq' .\qquad (25)$$

We have included the normalizing divisor in the definition of the integral equation, taking a step that is natural from the viewpoint of functional analysis (and computation). In the literature it is usual to impose normalization as a separate equation.

Equation (24) may be regarded as a nonlinear fixed-point problem $\rho = A(\rho)$ in an appropriate function space. For sufficiently small current I, the operator A is contractive, and a straightforward argument based on the contraction mapping principle leads to the following result:

Theorem : Suppose that the wake potential is bounded and continuous and satisfies the mild growth condition,

$$w = \sup_q \int_q^\infty du\ e^{-u^2/2} \left| \int_{q-u}^0 W(v)dv \right| < \infty ,\qquad (26)$$

and that the current parameter defined in (19) satisfies

$$I < \frac{(2\pi)^{1/2}}{we(1 + e)} ,\qquad (27)$$

where e is the base of the natural logarithm. Then (24) has a unique solution in the space of continuous functions ϕ such that

$$|\phi(q)| \leq \frac{e^{-q^2}}{2w} .\qquad (28)$$

This solution satisfies $\rho(q) \leq e^{-q^2}/((1+e)w)$, and it may be computed by functional iteration, $\rho^{(n+1)} = A(\rho^{(n)})$, beginning with any $\phi = \rho^{(0)}$ satisfying (28).

Thus, at sufficiently small current there is a unique equilibrium solution of the VFP equation that satisfies the detailed balance condition. The proof will be reported elsewhere [10]. In the above statement we have assumed that $W(q) = 0 , q > 0$. One may relax this condition and also allow W to have weak singularities [10].

8

It is remarkable that the equilibrium solution also provides an exact time dependent solution of the nonlinear Vlasov equation, namely (20) with the right hand side put to zero. With $f(q, p)$ as defined in (23) and ρ a solution of Haïssinski's equation, the following function solves the Vlasov equation:

$$g(q, p, \theta) = f(q - a \sin \theta, p - a \cos \theta) \ , \tag{29}$$

where $a > 0$ is arbitrary. That is, if the equilibrium solution is translated in phase space by *any* vector **a**, and the vector is rotated in time at the synchrotron frequency, the result is a solution of the time dependent Vlasov equation (but not of the full VFP equation). The proof is by substitution and a change of variable in the wake potential integral. For similar constructions for a different class of Vlasov equations see Lewis and Symon [29].

An inkling of this solution appears in the paper of Oide[14], which refers to a "trivial" dipole solution corresponding to motion of the center of mass of the bunch. However, the formula given in Eq.(10) of that paper is rather puzzling and does not correctly embody the physical idea. We are not inclined to call the result (29) trivial, on the contrary it seems surprising, and it is *not* a dipole mode in the usual sense. Conventionally, a dipole mode is the $m = 1$ angular Fourier component of a phase distribution that is rotating about the *origin* at the synchrotron frequency [28]. In polar coordinates such a distribution has the form $G(J, \phi - \theta)$. The solution g, with the displacement vector rotating, is quite a different thing. Of course, if we integrate (29) over p we get $\rho(q - a \cos \theta)$, so the charge density is just the equilibrium charge density oscillating as a rigid whole. It is tempting to call this a dipole motion, but for comparison to linear stability studies it is important to remember the distinction noted.

4   Solution of the VFP Equation for Longitudinal Dynamics

The wake potential W acounts for the electromagnetic environment of the beam comprised of various metalic structures in the vacuum chamber: bellows, flanges, transitions, kickers, etc. Bane and Ng [30] have carried out a detailed simulation of the wake potential for the SLC damping rings, using time domain electromagnetic codes. Since the ideal point source that defines W is not accessible numerically, the calculation was done with a short Gaussian bunch ($\sigma_z = 1$mm) as the source. Since 1mm is not extremely small compared to the actual bunchlength (5mm at low current) some small-wavelength fields that could affect the bunch dynamics are not excited in the simulation. Also, some of the difficult three dimensional structures had to be treated crudely. The result for the present damping ring vacuum chamber, which we use in our calculations, is shown in Figure 1. A comparison to results for the original vacuum chamber, replaced in 1992-93, will be given elsewhere [31]. Causality requires that the point source wake is zero in front of an ultrarelativistic bunch, whereas the computed wake, call it $\bar{W}$, has appreciable values in a small region with $q > 0$. Some authors arbitrarily truncate $\bar{W}$ to make it zero for $q > 0$. We prefer to use $\bar{W}$ as given, fearing that the truncation could produce spurious oscillations (as in the Gibbs phenomenon). In this
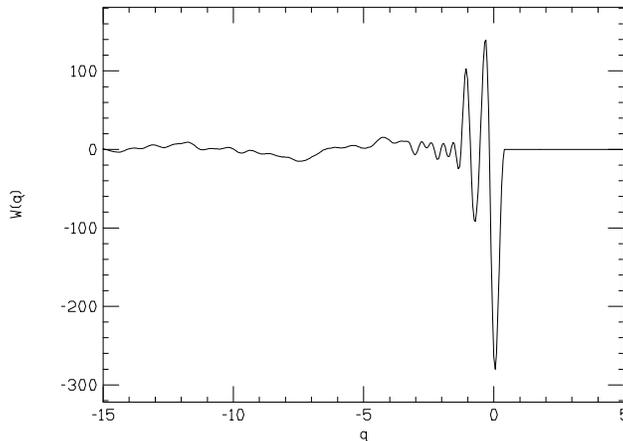
Figure 1: Wake potential $W(q)$ in Volts/picoCoulomb, for new damping ring vacuum chamber. $W > 0$ implies energy gain.

connection it is worthwhile to note the identity

$$\int_{-\infty}^{\infty} \bar{W}(q - q')\rho(q')dq' = \int_{-\infty}^{\infty} W(q - q')\bar{\rho}(q')dq' , \qquad (30)$$

where $\bar{\rho}$ is a smoothed version of ρ obtained by convolution with the Gaussian source of $\bar{W}$. Thus, for any distribution ρ, the error in the use of $\bar{W}$ as given amounts to taking out possible high frequency ripples in ρ (plus any errors in modeling $\bar{W}$ with the assumed Gaussian source).

We first solve the Haïssinski equation by a numerical method that does not require $W(q) = 0$, $q > 0$ (in contrast to the popular method based on integrating an associated differential equation). We simply approximate all integrals in (24) by a numerical integration rule (Simpson's method is quite adequate), thereby getting a system of nonlinear algebraic equations for the values $\rho(q_i)$, where $\{q_i\}$ is a finite uniform grid. These equations are solved by the matrix Newton method, taking the Gaussian $(2\pi)^{-1/2} \exp(-q_i^2/2)$ as the first guess. This works and converges rapidly up to fairly high current. For still higher current (far beyond the experimental values) one gets a solution by starting the Newton iteration at a linear extrapolation in current of the last good solution. From this success one infers that the solution is at least locally unique up to extremely high currents (say 50 times the currents experimentally achieved), since the Jacobian matrix of the system is always well-conditioned.

Figure 2 shows the Haïssinski solution at a current comparable to the experimental value for the threshold of bunch lengthening. Figure 3 shows the corresponding distorted potential well; i.e., the $q-$dependent part of the Hamiltonian. Streak camera measurements by Podobedov [32] have shown similar charge distributions in the subthreshold regime. This provides some confirmation of the wake potential and the VFP theory, but the experimental accuracy was not sufficient to distinguish the Bane-Ng wake potential from some simpler models. The existence of a locally unique solution of the Haïssinski equation at some current does not imply that the corresponding equilbrium is stable; a pendulum balanced at the top
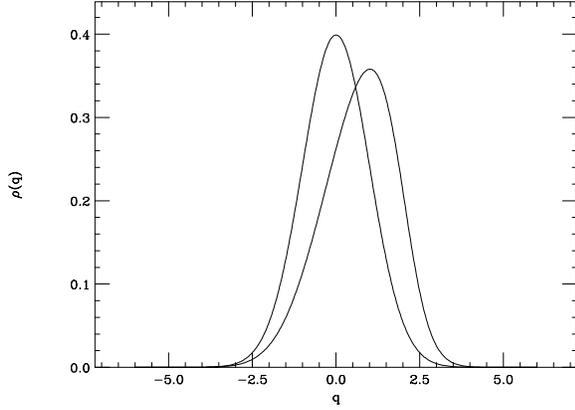
10

Figure 2: Calculated equilibrium charge distribution for $N = 1.64 \cdot 10^{10}$, and corresponding unperturbed distribution (for zero collective force).
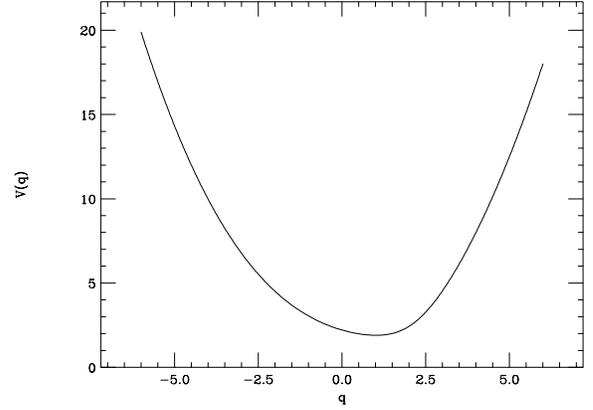
Figure 3: Distorted potential well for $N = 1.64 \cdot 10^{10}$.

of its swing is also in a locally unique equilibrium state. To study stability, we now turn to a direct time domain integration of the VFP equation, starting the integration at an accurate equilibrium solution from the Haïssinski equation.

We represent the distribution function $f(q, p, \theta)$ by polynomial interpolation of its values on a grid, $f_{ij}(\theta) = f(q_i, p_j, \theta)$. The task is to follow the f_{ij} as θ advances. We invoke operator splitting to treat the Vlasov and Fokker-Planck operators separately. First consider the effect of the Vlasov part alone. Given the inverse map $M^{-1} = M(\theta | \theta + \Delta\theta)$ for the single particle motion over a small step $\Delta\theta$, the propagation of the distribution is derived from

$$f(z_{ij}, \theta + \Delta\theta)) = f(M^{-1}(z_{ij}), \theta) , \quad z_{ij} = (q_i, p_j) . \tag{31}$$

The argument of f on the right side is not at a grid point, so the function must be evaluated by interpolation. We have tentatively adopted a biquadratic local interpolation (after finding some deficiencies of a bilinear interpolation). This is very easy to program and effective enough, but investigation of more refined schemes, for instance B-spline interpolation with higher smoothness, is on our agenda. To do the interpolation for any (i, j), we use a uniform Cartesian grid and first find the cell (k, l) in which $M^{-1}(z_{ij})$ lies. That is done quickly by taking integer parts of the two components of $M^{-1}(z_{ij})/\Delta$, where $\Delta = \Delta q = \Delta p$ is the grid step. Then define $(x, y) = (M^{-1}(z_{ij}) - z_{kl})/\Delta$, and use nine point biquadratic interpolation to evaluate (31). The result is the approximation

$$\begin{aligned}
4f_{ij}(\theta + \Delta\theta) = \\
x(x-1)[y(y-1)f_{k-1,l-1}(\theta) + 2(1-y^2)f_{k-1,l}(\theta) + y(y+1)f_{k-1,l+1}(\theta)] + \\
2(1-x^2)[y(y-1)f_{k,l-1}(\theta) + 2(1-y^2)f_{k,l}(\theta) + y(y+1)f_{k,l+1}(\theta)] + \\
x(x+1)[y(y-1)f_{k+1,l-1}(\theta) + 2(1-y^2)f_{k+1,l}(\theta) + y(y+1)f_{k+1,l+1}(\theta)] .
\end{aligned} \tag{32}$$

11

For a small step $\Delta\theta$ we take the map to be a composition of a rotation R through angle $\Delta\theta$ and a kick K of p at fixed q due to the wake field: $M(\theta + \Delta\theta|\theta) = K \circ R$. Hence

$$
\begin{aligned}
M(\theta|\theta + \Delta\theta)(z) &= R^{-1} \circ K^{-1}(z) \\
&= \left(\begin{array}{cc} \cos\Delta\theta & -\sin\Delta\theta \\ \sin\Delta\theta & \cos\Delta\theta \end{array} \right) \left(\begin{array}{c} q \\ p + IF(q, f(\cdot, \theta))\Delta\theta \end{array} \right) .
\end{aligned}
\tag{33}
$$

Since both K and R are symplectic, the resulting M is symplectic, hence volume preserving. Note that in interleaving rotations and kicks we have invoked operator splitting a second time. One can also view the algorithm as an Euler step in the interaction picture, regarding the harmonic oscillator as the unperturbed problem. It is likely that a higher order symplectic integrator will be more efficient than (33). Also, preliminary tests indicate that it is inefficient to update the distribution after every step of the map (33), although we have done so in the calculations reported here. Rather, one should take a few map steps between updates.

At each step the collective force (17) is evaluated by numerical integration, using the same grid and integration rule that was used for the Haïssinski solution. We first compute and store $\rho(q'_j)$, then do the integral against $W(q_i - q'_j)$ for each i.

The essentials of this method of integrating the Vlasov equation were introduced to plasma physics by Cheng and Knorr [20] in 1976. Their unperturbed problem was linear streaming rather than harmonic motion, and their interpolation method was different, but the basic idea of discretizing the local Perron-Frobenius operator was exactly the same. Recently Sonnendrücker *et al.* [21] have pursued the same technique, which they call a semi-Lagrangian method, in a plasma problem using a B-spline interpolation. Nakamura and Yabe [23] make the interesting observation that derivatives of the distribution can be propagated as well by the inverse map, and use that fact to put extra smoothness into a cubic interpolation scheme. They claim success in higher dimensional Vlasov plasma problems, which is certainly encouraging. None of these authors emphasize or even mention the importance of the symplectic condition, which we think to be important for faithful long-term modeling of any Hamiltonian system, with or without collective force. Also, these authors do not mention the connection to Perron-Frobenius theory . It is good to be aware of the connection, since that theory is undergoing interesting development in the field of mathematical dynamical systems [26, 33, 34, 35, 36] and numerical analysis [37].

To handle the Fokker-Planck (FP) term, we discretize it by divided differences, applying a formula suggested by Zorzano and Mais [38] in their work on the linear FP equation. With Δp denoting the grid step, the approximation at $z = (q_i, p_j)$ is

$$
\begin{aligned}
\frac{\partial}{\partial p}\left[pf + \frac{\partial f}{\partial p} \right] &\approx \frac{1}{\Delta p}[G_{i,j+1} - G_{i,j}] \\
G_{ij} &= \frac{1}{\Delta p}[f_{i,j} - f_{i,j-1}] + \frac{p_j}{2}[f_{i,j} + f_{i,j-1}] .
\end{aligned}
\tag{34}
$$

To propagate f by the FP operator, we compute a simple Euler step of the discretized form,

$$
\frac{1}{\Delta\theta}[f_{ij}(\theta + \Delta\theta) - f_{ij}(\theta)] = \frac{2\beta}{\Delta p}[G_{i,j+1}(\theta) - G_{i,j}(\theta)] .
\tag{35}
$$

Zorzano and Mais advocate a backward Euler method, which generally assures stability for a larger step $\Delta\theta$. Since our β is quite small (e.g., 0.001), and small β is equivalent to small $\Delta\theta$, the forward Euler method is found to be stable for our chosen $\Delta\theta$. The latter is determined by requirements of accuracy in the Vlasov step. We have tested the FP integration by turning off the collective force and comparing results to the analytic solution of the resulting FP equation for the harmonic oscillator [1].

Thanks to the representation (34) of the second order differential operator as a simple divided difference, the Euler step conserves total charge to high accuracy. That is, the numerical integral of the right side of (34) imitates the analytic integral over p of the left side, which is zero.

5   Numerical Results for Longitudinal Motion

We present results for the positron damping ring (SDR) of the SLC, and make comparisons to Podobedov's measurements reported in sections 4.2 and 4.3.3 of his thesis [32]. For these measurements (done with an r.f. voltage of 690 keV) the relevant machine parameters were

$$\sigma_E = 0.847 \text{ MeV} , \quad \sigma_z = 5.58 \text{ mm} ,$$
$$\nu_s = f_s/f_r = 0.01075 , \quad f_r = 8.5 \text{ MHz} ,$$
$$\beta = 1/\omega_s\tau_d = 9.78 \cdot 10^{-4} , \quad (\tau_d = \text{longitudinal damping time}) . \tag{36}$$

A complete list of machine parameters is on pp.54-55 of Podobedov. This list assumes an r.f. voltage of 800 keV, so some of the parameters are a bit different from those above. For the wake potential measured in volts/picoCoulomb, we quote I in corresponding units,

$$\frac{I}{N} = \frac{e^2}{2\pi\nu_s\sigma_E} = 2.80 \cdot 10^{-12} \text{ pC/V} . \tag{37}$$

We take a uniform Cartesian grid in phase space extending to 6σ of the unperturbed distribution; i.e., $q_i = 6i/n$, $i = -n, -n+1, \cdots, n$ and the same for p_i. We choose $n = 200$ for a 401×401 grid and take 1024 time steps per synchrotron period. There are 195 synchrotron periods in a damping time.

A run at any I begins with the Haïssinski equilibrium (23) for that I, computed to machine precision with the same grid, using Simpson's rule to define the integrals. We first report runs for I in a neighborhood of the threshold for bunch lengthening, namely for $N = (1.55 , 1.64 , 1.74) \cdot 10^{10}$. Figure 4 shows a plot of the dimensionless energy spread σ_p for each case, over a long time interval ($1.23\tau_d$, 240 synchrotron periods).

At $1.55 \cdot 10^{10}$ the equilibrium is apparently stable; at all times the computed distribution is indistinguishable on a plot from the original Haïssinski distribution. (On inspection of the numbers one sees a small discrepancy; the final bunch length and energy spread are about 1% smaller than initial values. It looks as though the time domain algorithm approaches its own equilibrium, slightly different from that of the Haïssinski equation.) Near invariance of the distribution for such a long time is already a gratifying success of the integration algorithm. It is by no means guaranteed that even an extremely precise approximation
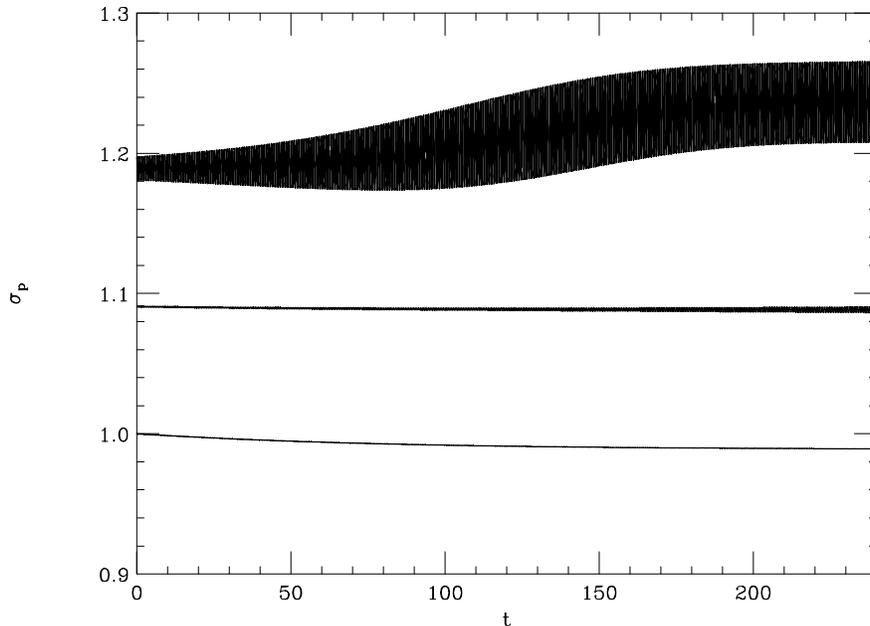
Figure 4: Time evolution of the dimensionless energy spread σ_p, for bunch populations $N = (1.55 \ , \ 1.64 \ , \ 1.74) \cdot 10^{10}$. The initial value is $\sigma_p = 1$ for each, but to separate the curves we have plotted $\sigma_p(1.55) \ , \ \sigma_p(1.64) + 0.1 \ , \ \sigma_p(1.74) + 0.2$. The time unit is one synchrotron period. The black band arises by fill-in from rapid oscillations, with frequency close to $2\omega_s$.

to the equilibrium will be maintained for a long time, since the time-stepping algorithm immediately introduces new approximations. Also, in all the runs of Figure 4 and in all runs discussed below (including some extending to four damping times with high current) the total charge is conserved to about one part in 10^5 and the distribution is very small at the edges of the grid (around 10^{-7} or smaller). We have used charge conservation and smallness at the edges as criteria in choosing the grid. Another test of the integration scheme is to reproduce the time dependent solution (29) of the Vlasov equation without Fokker-Planck terms. This was done successfully over a relatively short time span (a few synchrotron periods). The presence of the Fokker-Planck term seems to be essential for integrating stably to times comparable to the damping time. This does not necessarily mean that the method will fail in the case of proton beams, since there one deals with much lower peak current.

At $1.64 \cdot 10^{10}$ some small oscillations in σ_p show up at the largest times, and at $1.74 \cdot 10^{10}$ we see a quick build-up of large oscillations. We conclude that the equilibrium becomes unstable at about $N = 1.64 \cdot 10^{10}$. This is close to Podobedov's threshold for an instability signal; his Figure 46 gives about $1.7 \pm .03$ at 690 keV. Bane [39] has remarked that this close agreement may be fortuitous, since the addition of a slight amount of "missing" inductive wake field can, in his simulations [19], shift the threshold appreciably.

At currents just above threshold the simulation gives, after an initial long transient, sinusoidal oscillations of σ_p or σ_q at constant amplitude, with a frequency a bit lower than

$2\omega_s$. For instance, at $N = (1.74 , 1.84) \cdot 10^{10}$ this behavior sets in after about 2.5 damping times. At higher current there is a transition, apparently somewhat gradual, to a mode in which these oscillations have a slowly varying amplitude, a so-called "bursting" or "sawtooth" mode. At large times the envelope repeats periodically with a period comparable to the damping time. Figure 5 shows evolution of the bunch length for $N = 2.03 \cdot 10^{10}$, which seems to be near the computational bursting mode threshold. In this case an asymptotic periodicity is suggested, but is not yet exact at 3.7 damping times (720 periods). In experiment the transition to bursting seems to occur more precipitously, and at a higher current, around $2.6 \cdot 10^{10}$; see Ref.[32], Figure 43. Figure 6 shows the simulation at $2.99 \cdot 10^{10}$, the case that we examine in more detail below. Here a clear periodic behavior is established by 2.5 damping times. The noisy looking behavior around $t = 70$ is actually quite smooth when observed on an expanded t scale.
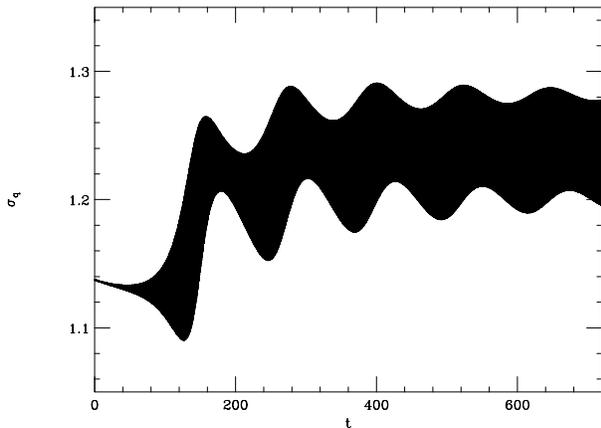

Figure 5: Time evolution of the dimensionless bunch length σ_q, for bunch population $N = 2.03 \cdot 10^{10}$. The time unit is one synchrotron period. The black band arises by fill-in from rapid oscillations, with frequency close to $2\omega_s$.
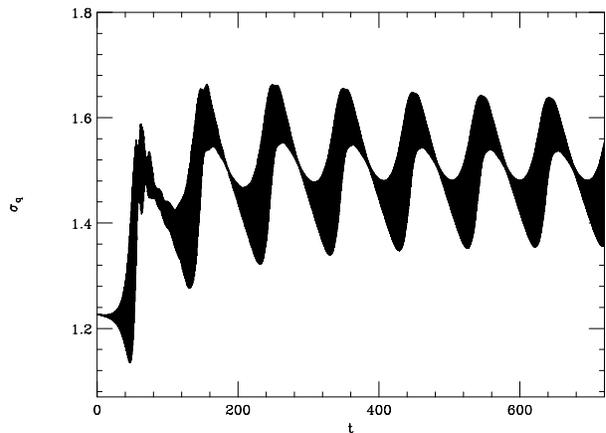
Figure 6: Time evolution of the dimensionless bunch length σ_q, for bunch population $N = 2.99 \cdot 10^{10}$. The time unit is one synchrotron period. A fairly clear periodic behavior sets in at about 2.5 damping times (500 synchrotron periods).

In the bursting mode at high current, the simulated distribution has a complicated time dependence, much different from the usual heuristic picture of a simple rotation in phase space of an almost rigid distribution. The charge distribution develops shoulders which come and go, move from left to right, etc. A series of typical snapshots is shown in Figure 7. Podobedov [32] has observed the charge distribution in detail with a streak camera. We shall compare his results to calculations in a later paper, and also explore contour plots of the phase space distribution.

Here we make a comparison to BPM data, which give an indirect picture of bunch oscillations. We first have to consider the relation of the BPM signal to the bunch form. Our discussion derives from the interesting treatment of Siemann [40]. His theory as it stands does not apply to our case of strong wake fields, but by abstracting some of his ideas we get an analysis that does apply. Part of our formulation was also noticed by Bane and Oide [19].
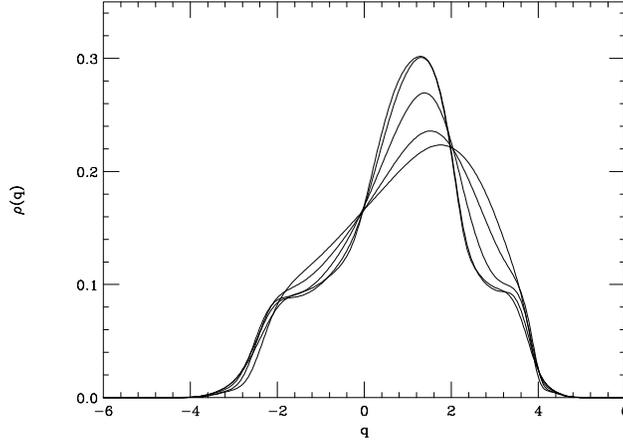
Figure 7: Typical snapshots of the charge distribution for bunch population $N = 2.99 \cdot 10^{10}$. The interval between snapshots is 6 synchrotron periods.

For this discussion it is convenient to use the variables $\tau = z/c$ and $t = \theta/\omega_s =$ time, in place of q and θ. We write λ for the charge density, so that

$$\lambda(\tau, t) = \frac{c}{\sigma_z} \rho(\frac{c\tau}{\sigma_z}, \ \omega_s t) \ . \tag{38}$$

Defining $T = 2\pi/\omega_r$ as the revolution time, we can represent the current at a reference point O in the beam position monitor as

$$\mathcal{I}(t) = eN \sum_{n=-\infty}^{\infty} \lambda(nT - t, nT) \ , \tag{39}$$

where the synchronous particle arrives at O at time nT , $n = 0, \pm 1, \cdots$. At a time $t = mT + \Delta t$ just after the arrival time mT of the synchronous particle, only one term in the sum contributes (if $\sigma_z \ll C$), and we have $\mathcal{I}(mT + \Delta t) = eN\lambda(-\Delta t, mT)$. The required value is actually $eN\lambda(-\Delta t, mT + \Delta t)$, but we can safely assume that the bunch does not deform during its transit time through the BPM, so that the two values are the same.

Since $\lambda(\tau, t)$ is a smooth and rapidly decaying function of τ, we can represent it as a Fourier integral,

$$\lambda(\tau, t) = \int_{-\infty}^{\infty} e^{i\omega\tau} \hat{\lambda}(\omega, t) d\omega \ . \tag{40}$$

We compute $\hat{\lambda}(\omega, t)$ from the VFP solution and find that it is periodic in t (at sufficiently large t), to good accuracy. Just above the instability threshold the period is a little more than twice the synchrotron frequency, whereas in the higher current bursting mode the period is much longer, about 6/10 of the damping time. Figure 8 shows one period of $\mathrm{Re}\hat{\lambda}(n\omega_r, t)$ in the latter situation, for $n = 1149$, a revolution harmonic at 9.8 GHz. Oscillations with the shorter period are superimposed on the long-period motion. In either case we can make a Fourier decomposition of the periodic motion with an appropriate period T_l:

$$\hat{\lambda}(\omega, t) = \sum_m e^{2\pi imt/T_l} \hat{\lambda}_m(\omega) \ . \tag{41}$$
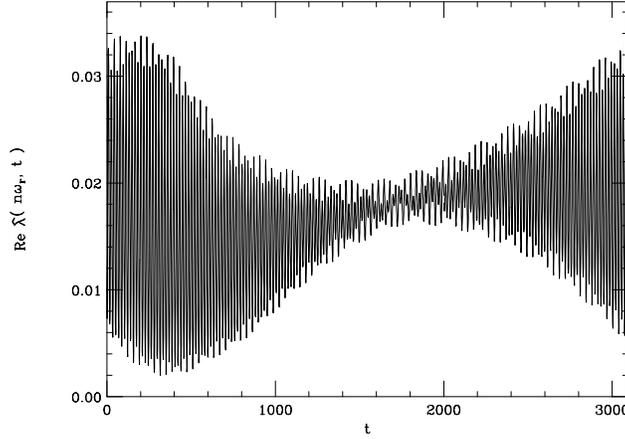
16

Figure 8: $\mathrm{Re}\hat{\lambda}(n\omega_r, t)$ versus t for $n = 1149$. The time unit is $1/32$ of the synchrotron period.

Since λ is real it is necessary that

$$\hat{\lambda}_{-m}(-\omega) = \hat{\lambda}_m(\omega)^* \ . \tag{42}$$

Substituting (41) and (40) in (39), and defining $\omega_l = 2\pi/T_l$, we find

$$\mathcal{I}(t) = eN \int d\omega e^{-i\omega t} \sum_m \hat{\lambda}_m(\omega) \sum_n e^{2\pi i n(m\omega_l + \omega)/\omega_r} \ . \tag{43}$$

The sum on n represents a periodic δ function. Recall that the Fourier inversion theorem (or Poisson's sum formula) may be expressed as

$$\frac{1}{b} \sum_n e^{2\pi i n\theta/b} = \sum_n \delta(\theta - nb) \ . \tag{44}$$

Applying this in (43) we get a formula expressing the frequency content of the BPM current,

$$\begin{aligned}
\mathcal{I}(t) =& \quad eN\omega_r \int d\omega e^{-i\omega t} \sum_m \hat{\lambda}_m(\omega) \sum_n \delta(m\omega_l + \omega - n\omega_r) \\
=& \quad eN\omega_r \sum_{m,n} e^{-i(n\omega_r - m\omega_l)t} \, \hat{\lambda}_m(n\omega_r - m\omega_l) \ .
\end{aligned} \tag{45}$$

The spectrum of the current consists of revolution harmonics $n\omega_r$ with sidebands $n\omega_r \pm m\omega_l$, $m = 1, 2, \cdots$. Although one is accustomed to the sidebands having equal amplitudes in the linear case [40](or even in the case in which the nonlinearity is only an amplitude-dependent tune), there is no reason to expect equal amplitudes in our case with full nonlinearity and a time-dependent potential well.

Figure 9 shows a plot of $|\hat{\lambda}_m(n\omega_r - m\omega_l)|^2$ versus $m\omega_l/\omega_s$ at fixed $n = 1149$, for the bursting mode at a bunch population $N = 2.99 \cdot 10^{10}$. The large amplitude of the revolution harmonic ($m = 0$) is off-scale and is not plotted. We see that there are quadrupole-like sidebands at distances $\pm 1.8\omega_s$ from the revolution harmonic, indeed with unequal amplitudes.
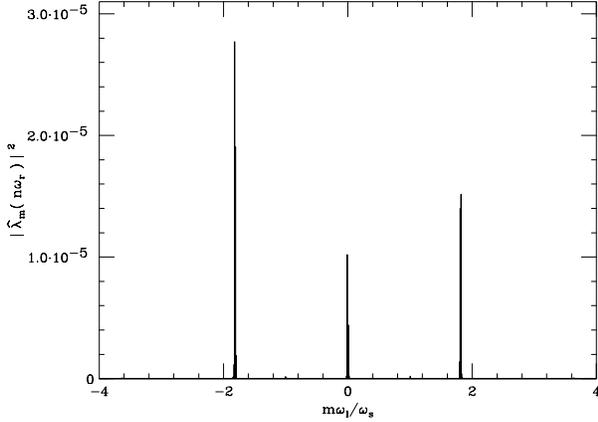
17

Figure 9: A bargraph of the spectral "power density", $|\hat{\lambda}_m(n\omega_r + m\omega_l)|^2$, versus $m\omega_l/\omega_s$ for $n = 1149$. There are six large mode amplitudes, for $m = \pm(175, 176)$ and $m = \pm 1$. The large amplitude of the revolution harmonic $m = 0$ is off scale and is not plotted.
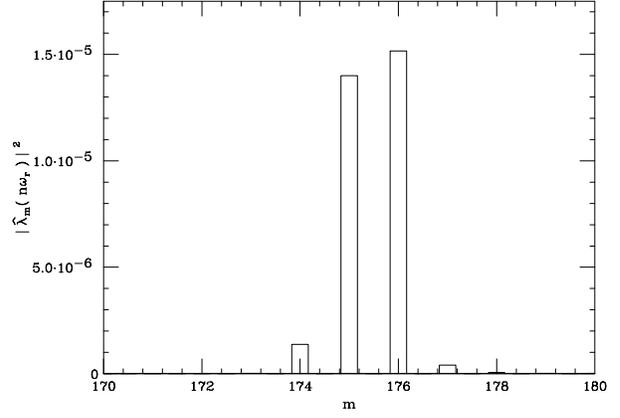
Figure 10: An enlarged bargraph of the upper sideband spectral density versus m, showing large modes at $m = 175$, 176 and small modes at 174, 177.

Each sideband actually contains two large neighboring modes, as seen in Figure 10. The large modes are at $m = \pm(175$, $176)$ with frequencies

$$m\omega_l = \pm(\ 1.8105\ ,\ 1.8209\ )\omega_s\ . \tag{46}$$

There are also large low-frequency modes at $m = \pm 1$, and a few weak modes that have little effect. The variation of the envelope in Figure 8, the "bursting" behavior, arises from beating of 175 against 176 (and -175 against -176). The beat frequency is just ω_l, the same as the frequency of the modes $m = \pm 1$. Consequently, if we leave the latter out of the Fourier series for $\hat{\lambda}(n\omega_r, t)$, the only effect is to subtract a sinusoid with the same wavelength as the envelope (perhaps shifted in phase). As shown in Figure 11, that does not change the qualitative picture.

The frequency of the rapid oscillations is the average of the two frequencies of (46), or $1.8157\omega_s$. The spectral analysis of BPM data, shown in Figure 41 of Ref.[[32]] gives $(1.84 \pm .02)\omega_s$. (Here we have guessed the experimental error from the contour plot of Figure 41). One's delight in the good agreement is tempered by the fact that experiment shows a second spectral line, at $2.54\omega_s$, at a current only slightly higher, say $3.2 \cdot 10^{10}$. We find no such thing as we increase the current, nor do we see the observed disappearance of the bursting mode at around $3.3 \cdot 10^{10}$. Rather, our bursting mode with fast oscillations around $1.8\omega_s$ persists up to $3.93 \cdot 10^{10}$, the highest current of our simulations to date.

The BPM current is not measured directly, rather one measures the voltage at the end of the cable leading to the BPM. If $Z(\omega)$ is the impedance of the BPM and cable together, the Fourier transform of the measured voltage is

$$\hat{\mathcal{V}}(\omega) = Z(\omega)\hat{\mathcal{I}}(\omega) = Z(\omega)eN\omega_r \sum_m \hat{\lambda}_m(\omega) \sum_n \delta(m\omega_l + \omega - n\omega_r)\ , \tag{47}$$
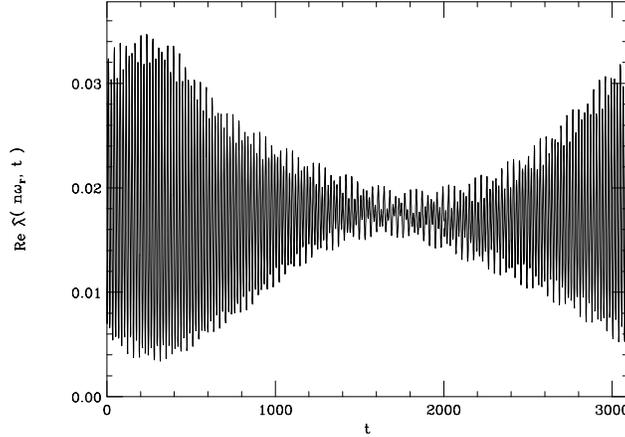
18

Figure 11: $\text{Re}\hat{\lambda}(n\omega_r, t)$ versus t for $n = 1149$, with the modes $m = \pm 1$ omitted from its Fourier series. The unit of t is $1/32$ of the synchrotron period.

hence

$$\mathcal{V}(t) = eN\omega_r \sum_{m,n} e^{-i(n\omega_r - m\omega_l)t} Z(n\omega_r - m\omega_l)\hat{\lambda}_m(n\omega_r - m\omega_l) \ . \tag{48}$$

One can see an instability signal in $\mathcal{V}(t)$ by a frequency analyzer set to receive a sideband of a relevant revolution harmonic. Podobedov and Siemann devised a demodulation method that uses many revolution harmonics to achieve a better signal-to-noise ratio [41]. They first apply a 10 GHz high-pass filter (mostly to reduce the power level to a manageable value) then put the signal through a square-law detector (diode) which squares it to good accuracy. The signal is then amplified (40db) and sent through a 5 MHz low-pass filter, and finally to an oscilloscope (through "a.c. coupling", meaning that the d.c. component is removed). If F_1 represents the high-pass filter, and F_2 the low-pass filter plus removal of d.c., the oscilloscope signal is

$$S(t) = \alpha(\mathcal{V}_{F_1}^2)_{F_2} \ , \tag{49}$$

where α is a factor (assumed to be frequency-independent) to account for the change in signal level in the diode and amplifier.

For $\mathcal{V}_{F_1}$ we have (48) with the sums restricted to $|n\omega_r| > 2\pi(10\text{GHz})$ and $|m\omega_l| \leq 4\omega_s$, there being no significant components for larger m. We define the corresponding domains as $|n| > \underline{n}$ and $|m| < \overline{m}$. It seems safe also to set $Z(n\omega_r - m\omega_l) = Z(n\omega_r)$ and $\hat{\lambda}_m(n\omega_r - m\omega_l) = \hat{\lambda}_m(n\omega_r)$ since $|m\omega_l/n\omega_r| < 4 \cdot 10^{-5}$. Indeed, we have validated this approximation for $\hat{\lambda}$ in our simulation. Separating the $m = 0$ terms and defining $\kappa = (eN\omega_r)^2$, we have

$$\mathcal{V}_{F_1}(t)^2 = \mathcal{V}_{F_1}(t)\mathcal{V}_{F_1}^*(t)$$

$$= \kappa \sum_{|n|>\underline{n}} Z(n\omega_r)\left[\hat{\lambda}_0(n\omega_r)e^{-in\omega_r t} + \sum_{0<|m|<\overline{m}} \hat{\lambda}_m(n\omega_r)e^{-i(n\omega_r - m\omega_l)t}\right]$$

$$\times \sum_{|n'|>\underline{n}} Z(n'\omega_r)^*\left[\hat{\lambda}_0(n'\omega_r)^*e^{in'\omega_r t} + \sum_{0<|m'|<\overline{m}} \hat{\lambda}_{m'}(n'\omega_r)^*e^{i(n'\omega_r - m'\omega_l)t}\right] . \tag{50}$$

Of the various terms in the product (50), the d.c. terms are taken out by F_2, as are all terms with frequencies of the form $(n' - n)\omega_r - (m' - m)\omega_l$, $n \neq n'$, since $f_r = 8.5\text{MHz} > 5\text{MHz}$ and $|m' - m|\omega_r$ is small compared to $n\omega_r$. Thus, the oscilloscope signal is

$$S(t) = S_1(t) + S_2(t) - \langle S_2 \rangle , \tag{51}$$

where

$$S_1(t) = 2\alpha\kappa\text{Re}\left[\sum_{|n|>\underline{n}} |Z(n\omega_r)|^2 \sum_{0<|m|<\overline{m}} \hat{\lambda}(n\omega_r)_0^*\hat{\lambda}(n\omega_r)_m e^{im\omega_l t}\right] , \tag{52}$$

$$S_2(t) = \alpha\kappa \sum_{|n|>\underline{n}} |Z(n\omega_r)|^2 \sum_{0<|m|,|m'|<\overline{m}} \hat{\lambda}_m(n\omega_r)\hat{\lambda}_{m'}(n\omega_r)^*e^{i(m-m')\omega_l t} , \tag{53}$$

and $\langle S_2 \rangle$ is the d.c. component of S_2.

Since our computation shows that $\hat{\lambda}_0(n\omega_r)$ is large compared to $\hat{\lambda}_m(n\omega_r)$, $m \neq 0$, the term S_1 is the dominant part of the signal. This term was of course emphasized in the invention of the diode demodulation method [41], and it was called the "instability signal". A contribution to S_1 for a single n is proportional to the real part of $\hat{\lambda}(n\omega_r, t)$, the Fourier transform of the bunch form with respect to τ at that n.

It turns out, however, that S_2 is not negligible, so that the pure instability signal will not be seen in the oscilloscope trace. The contribution to S_2 for a given n is proportional to the square of the instability signal for that n. In the simulation, S_2 is responsible for the asymmetry between the upper and lower envelopes of the oscilloscope trace. An asymmetry is also seen in the data but was not previously associated with S_2. Figure 12 shows the simulated oscilloscope trace in arbitrary units for $N = 2.99 \cdot 10^{10}$, including all revolution harmonics nf_r between 9.8 and 20 GHz ($1149 \leq n \leq 2352$), and assuming that the BPM impedance $|Z(n\omega_r)|$ is independent of n. The 20 GHz cut-off was chosen since there seems to be significant unfiltered BPM signal up to that frequency. Figure 13 shows the corresponding experimental graph from Ref.[41], kindly provided by the authors. The period of the bursting envelope is $0.607\tau_d$ in the calculation and about $0.62\tau_d$ as read from the experimental graph for $3.1 \cdot 10^{10}$.

Actually, the BPM impedance is not expected to be constant over such a large range of frequencies; it may in fact show resonant peaks or high-frequency fall-off that could change the oscilloscope trace in comparison to Figure 12. Its absolute value can be measured
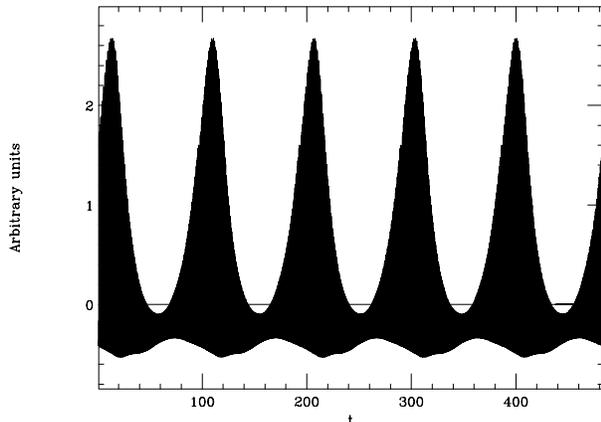
Figure 12: Simulated oscilloscope trace for $N = 2.99 \cdot 10^{10}$, in arbitrary units. The time unit is one synchrotron period. The straight line gives the mean value of the plotted data, zero as it ought to be.
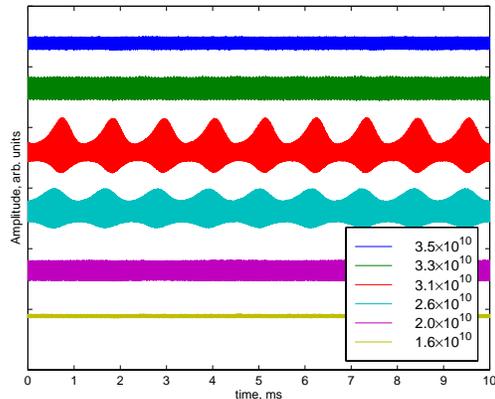

Figure 13: Experimental oscilloscope traces for various currents. The third curve from the top is for $N = 3.1 \cdot 10^{10}$.

by doing a frequency analysis of the BPM signal, with no filter over the required range of revolution harmonics, at low current where the bunch form is well known. Once this relatively easy measurement is performed, we can make a a more complete comparison of theory to experiment.

6   Summary and Outlook

We have presented a method for stable long-term integration of the nonlinear Vlasov-Fokker-Planck equation. Applied to the SLC positron damping ring, it yields several aspects of observed bunch behavior for bunch population up to $3 \cdot 10^{10}$. The threshold of bunch lengthening, the frequency of bunch oscillations, and the period of the bursting envelope are all in good agreement with experiment. The computed threshold for the bursting mode appears to be somewhat low, although we have not yet determined it exactly, and we do not know how to judge experimental sensitivity to this mode. Observed phenomena for $N \geq 3.2 \cdot 10^{10}$ are not reproduced, in particular the disappearance of the bursting mode and appearance of a spectral line at $2.5\omega_s$. Comparisons with streak camera measurements are yet to be made.

Many interesting questions remain to be explored, both in longitudinal bunch motion and in wider applications of VFP equations. For longitudinal motion we should strive to understand the results in intuitive terms, perhaps by abstracting a simpler model after a detailed examination of the numerical data. The association of bursting with beats between neighboring Fourier modes in the time dependence of the bunch form is intriguing, and should be analyzed. We should also try to understand the effect of changes in the wake potential. This would have the short range goal of resolving conflicts of theory and experiment, and the long range goal of trying to prevent bursting behavior in practice. Long-period "relaxation"

21

oscillations, some noticeably different from the SLC bursting mode, have been seen at several machines [42, 43, 44, 45]. Perhaps our method will help to sort out these varied phenomena. There have been theoretical ideas [46, 47, 48, 49, 45, 50, 51] and simulations [52, 53, 19] on the subject going back to 1981.

The computations were done with modest computing power, stringing together several long runs on work stations to integrate for 2-4 damping times. A run of 120 synchrotron periods $(.61\tau_d)$ takes 17 hours on an IBM RISC 6000 with 200 MHz clock. For greater convenience or for extension of the method to more degrees of freedom we need a substantial speed-up. We are certain that there is ample opportunity for a big improvement in the algorithm, still staying with the basic idea. The problem is well suited to parallel computation, since the single-particle tracking and interpolations associated with different grid points can be done independently on different processors.

In pursuit of other applications of the method, we have already applied it to the coherent beam-beam interaction ("strong-strong" model) in one degree of freedom. Although this involved two coupled VFP equations, the computation proved to be easier than the one reported here, and resulted in discovery of an apparent equilibrium state. We then formulated an integral equation for the equilibrium, generalizing the Haïssinski equation to a case in which the Hamiltonian has explicit time dependence. Since the integral equation has a unique solution at small current, we have settled the long standing question of existence of an equilibrium for this model [13].

If one can successfully implement the method in two or three degrees of freedom, there will be a much longer list of interesting applications. This would include single-pass problems such as the matching of a space-charge dominated beam to a focusing channel in a linac. For this an integral equation to express the matching condition might also be of interest.

Acknowledgments

References

[1] S. Chandrasekhar, *Rev. Mod. Phys.* **15**, 1 (1943), reprinted in *Noise and Stochastic Processes*, ed. N. Wax (Dover, New York, 1954).

[2] C. W. Gardiner, *Handbook of Stochastic Methods* (Springer, Berlin, 1983).

[3] H. Risken, *The Fokker-Planck Equation* (Springer, Berlin, 1989).

[4] C. Soize, *The Fokker-Planck Equation for Stochastic Dynamical Systems and its Explicit Steady State Solutions* (World Scientific, Singapore, 1994).

[5] T. C. Gard, *Introduction to Stochastic Differential Equations* (M. Dekker, New York, 1988).

[6] L. Arnold, *Stochastic Differential Equations: Theory and Applications* (Wiley, New York, 1974).

[7] J. M. Jowett, in *Nonlinear Dynamics Aspects of Particle Accelerators*, Lect. Notes in Phys., V.247 (Springer, Berlin, 1986).

[8] G. Ripken and E. Karantzoulis, DESY HERA 92-05 (1992) and DESY 90-135 (1990); D .P. Barber, K. Heinemann, H. Mais, G. Ripken, DESY 91-146 (1991).

[9] J. Haïssinski, *Nuovo Cimento* **18 B**, 72 (1973).

[10] R. Warnock *et al.*, in preparation.

[11] S. Ivanov, CERN/SL/90-19(AP) (1990).

[12] F. Bouchut and J. Dolbeault, *Diff. and Int. Eq.* **8**, 487 (1995).

[13] J. Ellison and R. Warnock, in preparation.

[14] K. Oide, *Proc. 4th Advanced ICFA Beam Dynamics Workshop*, p.64 (KEK, Tsukuba, Japan, 1991); K. Oide and K. Yokoya, KEK-Preprint-90-10 (1990).

[15] G. R. Bart and R. L. Warnock, *SIAM J. Math. Anal.* **4**, 609 (1973); G. R. Bart, *J. Math. Anal. and Appl.* **79**, 48 (1981).

[16] N. G. van Kampen, *Physica* **21**, 949 (1955); K. M. Case, *Annals of Physics, NY* **7**, 349 (1959) and *ibid.* **9**, 1 (1960); for mathematical aspects see D. H. Sattinger, *J. Math. Anal. and Appl.* **15**, 497 (1966).

[17] J. K. Koga and T. Tajima, *J. Comp. Physics* **116**, 314 (1995).

[18] R. W. Hockney and J. W. Eastwood, *Computer Simulation Using Particles* (Adam Hilger, Bristol, 1988).

[19] K. L. F. Bane and K. Oide, *Proc. 1995 IEEE Part. Accel. Conf., Dallas, Texas* and *Proc. 1993 IEEE Part. Accel. Conf., Washington, DC.*

[20] C. Z. Cheng and G. Knorr, *J. Comp. Phys.* **22**, 330 (1976).

[21] E. Sonnendrücker, J. Roche, P. Bertrand, and A. Ghizzo, *J. Comp. Phys.* **149** , 201 (1999).

[22] H. Ruhl, proceedings of *Nonlinear and Stochastic Beam Dynamics in Accelerators*, Lüneburg, Germany, 1997 , DESY 97-161.

[23] T. Nakamura and T. Yabe, *Comp. Phys. Commun.* **120**, 122 (1999).

[24] R. C. Davidson, H. Qin, P. H. Stoltz, and T.-S. F. Wang, *Phys. Rev. ST - AB* **2**, 054401-2 (1999); P. H. Stoltz, R. C. Davidson, and W. Wei-li Lee, *Phys. Plasmas* **6**, 298 (1999).

[25] P. Channell, *Phys. of Plasmas* **6**, 982 (1999).

[26] A. Lasota and M. C. Mackey, *Chaos, Fractals, and Noise* (Springer, New York, 1994).

[27] M. Sands, *The Physics of Electron Storage Rings - an Introduction*, SLAC-121, Eq. 5.64 (1970).

[28] A. Chao, *Physics of Collective Beam Instabilities in High Energy Accelerators*, Eqs. (4.1)-(4.2) (Wiley, New York, 1993).

[29] H. R. Lewis and K. R. Symon, *Phys. Fluids* **27**, 192 (1984).

[30] K. Bane and C.-K. Ng, Proc. 1993 IEEE Part. Accel. Conf., Washington, D.C., p.3432.

[31] R. Warnock and K. Bane, Proc. 2000 Euro. Part. Accel. Conf., Vienna, Austria.

[32] B. V. Podobedov, *Saw-Tooth Instability Studies at the Stanford Linear Collider Damping Rings*, Ph.D. Thesis, Stanford University, SLAC-Report-543 (1999).

[33] D. J. Driebe, *Fully Chaotic Maps and Broken Time Symmetry* (Kluwer, Dordrecht, 1999).

[34] P. Deuflhard, M. Dellnitz, O. Junge, and Ch. Schütte, in *Computational Molecular Dynamics: Challenges, Methods, Ideas*, P. Deuflhard *et al.*, eds. (Springer, Berlin, 1998); M. Dellnitz and O. Junge, *SIAM J. Num. Anal.* **36**, 2 (1999). See also other papers by some of the same authors on the Web sites http://www.zib.de/bib/pub/pw/index.de.html and http://math-www.uni-paderborn.de/ agdellnitz/publications/index.html. In this work eigenvectors of the PF operator with eigenvalue close to 1 are discussed; these correspond to quasi-equilibrium states, and may be of interest for the beam matching problem.

[35] M. Keane, R. Murray, and L.-S. Young, *Nonlinearity* **11**, 27 (1998).

[36] F. Y. Hunt, *Nonlinearity* **11**, 307 (1998).

[37] J. Ding, Q. Du, and T. Y. Li, *Appl. Math. and Comp.* **53**, 151 (1993).

[38] M. P. Zorzano and H. Mais, Proc. 1998 IEEE Part. Accel. Conf., p.1825.

[39] K. Bane, private communication.

[40] R. Siemann, in *Physics of Particle Accelerators*, Vol.1, AIP Conf. Proc. **184** (Amer. Inst. Phys., New York, 1989).

[41] B. Podobedov and R. Siemann, Proc. 1999 IEEE Part. Accel. Conf., p.146.

[42] K. C. Harkay and N. S. Sereno, National Institute of Standards and Technology report LS-268.

[43] K. C. Harkay, M. Borland, Y.-C. Chae, L. Emery, Z.Huang, E. S. Lessner, A. H. Lumpkin, S. V. Milton, N. S. Sereno, and B. X. Yang, Proc. 1999 IEEE Part. Accel. Conf., New York, p.1644.

[44] R. Nagaoka, J. L. Revol, P. Kernel, and G. Besnier, Proc. 1999 IEEE Part. Accel. Conf., New York, p.1192.

[45] C. Limborg and J. Sebek, *Phys. Rev. E* **60**, 4823 (1999).

[46] Y. Chin and K. Yokoya, *Nucl. Instr. Meth. Phys. Res.* **226**, 223 (1984).

[47] M. D'yachkov, *Longitudinal Instabilities of Bunched Beams Caused by Short-Range Wake Fields*, Ph.D. thesis, University of British Columbia (1995).

[48] G. V. Stupakov, B. N. Breizman, and M. S. Pekker *Phys. Rev. E* **55**, 5976 (1997).

[49] S. Heifets and B. Podobedov, *Phys. Rev. ST-AB* **2**, 044402-1 (1999).

[50] M. Migliorati, L. Palumbo, G. Dattoli, and L. Mezi, 1999 IEEE Part. Accel. Conf., p.1219.

[51] A. Moisnier, 1999 IEEE Part. Accel. Conf., New York, p.1662.

[52] T. Weiland, DESY 81-88 (1981).

[53] R. Baartman and M. D'yachkov, 1995 IEEE Part. Accel. Conf., p. 3119.